Performance Evaluation of Downlink Beamforming over Non-Stationary Channels with Interference

Adrian Ispas*, Christian Schneider†, Gerd Ascheid*, and Reiner Thomä†

*Chair for Integrated Signal Processing Systems, RWTH Aachen University, Germany

{ispas, ascheid}@iss.rwth-aachen.de

†Institute of Information Technology, Ilmenau University of Technology, Germany

{christian.schneider, reiner.thomae}@tu-ilmenau.de

Abstract—**Interference is one of the major bottlenecks in current cellular networks. A realistic evaluation of the achievable performance in interference-limited systems based on measured channels is thus necessary; however, only few results are known from literature. We evaluate the achievable performance in a cellular network with inter-cell interference based on measured channels in an urban macrocell scenario at 2.53 GHz. To this end, the mutual information is introduced as an appropriate performance measure over fast and slow fading channels that are non-stationary but doubly underspread. We discuss appropriate channel normalizations and the limitations of an evaluation based on sequential measurements. Moreover, we analyze the accuracy of an approximate but commonly used evaluation of the mutual information. A second-order multivariate Taylor series expansion reveals the signal and interference contributions to the approximation error. We find that the approximation is accurate in realistic ICI scenarios.**

I. INTRODUCTION

Inter-cell interference (ICI) is the main performance limitation in current cellular networks [1]; this is especially a concern for mobile terminals (MT) at the cell-edge. A promising approach to mitigate interference and thus to improve the system performance while achieving fairness among all MTs in the network is the use of transmit beamforming with multiple antennas at each base station (BS) [2], [3]. Furthermore, in any realistic communication system the channel is non-stationary in time, i.e., the statistics of the channel process change over time [4], [5]. In order to obtain a realistic performance evaluation, interference and the non-stationarity of the channel must be properly modeled using measured channels. These two aspects are only unsatisfactorily modeled in current system-level simulation environments and thus require additional attention for a realistic performance analysis [6]–[8].

The mutual information (MI) over multiple-input and multiple-output (MIMO) channels with ICI and single-user detection (SUD) is given in, e.g., [9], [10]. These contributions have investigated the ergodic capacity and optimum signaling schemes for Rayleigh and Rician frequency-flat fading channels, respectively. Furthermore, [10] has derived an approximate expression for the MI that allows for a simplified analysis. Only few measurement-based results on the MI or related quantities for the ICI case with SUD are known. In [11] and [12], the performance over measured urban macrocell channels with ICI and SUD has been evaluated. The MI of frequency-flat fading MIMO channels in a slow fading scenario has

been investigated in [11] based on measurements at 2.53 GHz. In [12], average weighted sum rates of coordinated multicell techniques for frequency-flat fading multiple-input and single-output (MISO) channels have been evaluated at 1.8 GHz.

Contributions: We characterize the achievable performance in an ICI-limited cellular network where each BS performs downlink beamforming to a single MT per time slot over a time-selective, frequency-flat fading channel. The performance evaluation is based on non-stationary, doubly underspread (DU) [13] channels measured in an urban macrocell scenario that is relevant to 3GPP Long Term Evolution (LTE). Our main contributions are as follows.

- We introduce the MI as appropriate performance measure for fast and slow fading channels that are non-stationary but DU. Furthermore, we discuss the limitations of an evaluation of the MI based on sequential measurements.
- We give a detailed evaluation of the MI for two types of channel normalizations; the results can be compared to values obtained from simulation and they serve as baseline values for ICI-mitigating beamforming techniques.
- We analyze the accuracy of a commonly used approximation of the MI and characterize the signal and ICI contributions to the approximation error. We show that the approximation is accurate in realistic ICI scenarios, especially at the cell-edge.

Notation: $\mathbf{A}^*$, $\mathbf{A}^T$, and $\mathbf{A}^H$ denote the (element-wise) complex conjugate, the transpose, and the conjugate transpose of the matrix $\mathbf{A}$, respectively. $||\mathbf{A}||_F$ denotes the Frobenius norm of the matrix $\mathbf{A}$. The expectation of a random value x is denoted by $\mathrm{E}\{x\}$. The $N \times N$ identity matrix is represented by $\mathbf{I}_N$. All logarithms are to the base 2 unless otherwise specified.

II. SYSTEM MODEL

We consider a downlink ICI network with N_{BS} BSs where one BS transmits to a single MT per time slot. The ICI results from $N_{\mathrm{BS}} - 1$ BSs transmitting each to a single and different MT per time slot. We assume that transmission is taking place over a time-varying and frequency-flat fading MISO channel with N_{TX} antennas at each BS and a single antenna at the MT. Furthermore, the BSs use local statistical knowledge about the channel, i.e., each BS i has only statistical channel knowledge about the link to its MT to perform transmit beamforming. In the complex baseband, the matched-filtered and symbol-sampled received signal at the MT associated to BS k is

expressed as

$$y_k[m] = \mathbf{L}_{\mathrm{H},k,k}[m]\mathbf{w}_k[m]x_k[m]$$
$$+ \sum_{i=1,i\neq k}^{N_{\mathrm{BS}}} \mathbf{L}_{\mathrm{H},k,i}[m]\mathbf{w}_i[m]x_i[m] + n_k[m] \quad (1)$$

for the time slot $m \in \mathbb{Z}$. The samples $\mathbf{L}_{\mathrm{H},k,i}[m]$ are jointly proper row vectors containing the random fading values of the MISO channel from BS i to the MT associated to BS k. We assume the receiver to perform SUD and to have CSI, i.e., the MT associated to BS k has knowledge of the current channel realizations $\mathcal{L}_{\mathrm{H},k}[m] = \{\mathbf{L}_{\mathrm{H},k,i}[m] \mid i = 1,\ldots,N_{\mathrm{BS}}\}$. The beamforming weights $\mathbf{w}_i[m]$ of BS i fulfill $||\mathbf{w}_i[m]||_F^2 = 1$. The samples $x_i[m]$ are uncorrelated jointly proper Gaussian signals sent from BS i with power $\mathrm{E}\{|x_i[m]|^2\} = \sigma_{x,i}^2[m]$; the signals of the BSs are mutually independent. The samples $n_i[m]$ denote white jointly proper Gaussian noise with power σ_n^2. We define the instantaneous signal-to-noise ratio (SNR) for the MT associated to BS k as $\rho_k[m] = \rho_{k,k}[m]$ where $\rho_{k,i}[m]$ is the instantaneous interference-to-noise ratio (INR) for the MT associated to BS k due to ICI from BS i:

$$\rho_{k,i}[m] = \frac{||\mathbf{L}_{\mathrm{H},k,i}[m]||_F^2}{N_{\mathrm{TX}}}\frac{\sigma_{x,i}^2[m]}{\sigma_n^2}. \quad (2)$$

Note that these definitions of the SNR and the INR do not contain beamforming gains.

III. MUTUAL INFORMATION WITH BEAMFORMING

With respect to (w.r.t.) the system model in Section II, the MI between the input at BS k and the corresponding output combined with CSI at the receiver is given by [9]

$$I_{\mathrm{BF}}(x_k[m]; y_k[m], \mathcal{L}_{\mathrm{H},k}[m])$$
$$= \mathrm{E}\left\{\log\left(1 + \mathbf{L}_{\mathrm{H},k}[m]\mathbf{Q}_k[m]\mathbf{L}_{\mathrm{H},k}^H[m]z_k^{-1}[m]\right)\right\} \quad (3)$$

with $\mathbf{L}_{\mathrm{H},k}[m] = \mathbf{L}_{\mathrm{H},k,k}[m]$, the input covariance matrix of BS i denoted by $\mathbf{Q}_i[m] = \mathbf{w}_i[m]\mathbf{w}_i^H[m]\sigma_{x,i}^2[m]$, and $z_k[m] = \sum_{i=1,i\neq k}^{N_{\mathrm{BS}}} \mathbf{L}_{\mathrm{H},k,i}[m]\mathbf{Q}_i[m]\mathbf{L}_{\mathrm{H},k,i}^H[m] + \sigma_n^2$.

A. Statistical Beamforming

BS k performs (non-cooperative) beamforming to the MT associated to it based on statistical knowledge of the corresponding link with $\mathbf{w}_k[m] = \mathbf{u}_{\mathrm{max},k}^*[m]$. Here $\mathbf{u}_{\mathrm{max},k}[m]$ is the dominant eigenvector of $\mathbf{R}_k[m] = \mathbf{R}_{k,k}[m]$ and $\mathbf{R}_{k,i}[m] = \mathrm{E}\{\mathbf{L}_{\mathrm{H},k,i}^T[m]\mathbf{L}_{\mathrm{H},k,i}^*[m]\}$ is the correlation matrix of the channel from BS i to the MT associated to BS k. Assuming only knowledge of $\mathbf{R}_k[m]$ at BS k, with this technique, each BS maximizes the (average) signal power at its MT while disregarding any interference to MTs associated to other BSs.

B. Approximate Evaluation of the Mutual Information

In [10], an approximate evaluation of the MI (3) is given for independent elements of $\mathcal{L}_{\mathrm{H},k}[m]$; it can be slightly simplified for a MISO channel [3]:

$$I_{\mathrm{BF}}(x_k[m]; y_k[m], \mathcal{L}_{\mathrm{H},k}[m])$$
$$\approx \log\det\left(\mathbf{I}_{N_{\mathrm{TX}}} + \mathrm{E}\left\{\mathbf{L}_{\mathrm{H},k}^H[m]\,\mathrm{E}\{z_k[m]\}^{-1}\mathbf{L}_{\mathrm{H},k}[m]\right\}\mathbf{Q}_k[m]\right)$$
$$= \log\det\left(\mathbf{I}_{N_{\mathrm{TX}}} + \mathrm{E}\{z_k[m]\}^{-1}\mathbf{R}_k^*[m]\mathbf{Q}_k[m]\right)$$
$$= \log\left(1 + \mathrm{SINR}_k[m]\right). \quad (4)$$

We used the equality $\det(\mathbf{I}_M + \mathbf{AB}) = \det(\mathbf{I}_N + \mathbf{BA})$ for matrices $\mathbf{A}$ and $\mathbf{B}$ of appropriate sizes. Furthermore, we defined the signal-to-interference-plus-noise ratio (SINR) of the MT associated to BS k as

$$\mathrm{SINR}_k[m] = \frac{\mathbf{w}_k^H[m]\mathbf{R}_k^*[m]\mathbf{w}_k[m]\sigma_{x,k}^2[m]}{\sum_{i=1,i\neq k}^{N_{\mathrm{BS}}}\mathbf{w}_i^H[m]\mathbf{R}_{k,i}^*[m]\mathbf{w}_i[m]\sigma_{x,i}^2[m] + \sigma_n^2}. \quad (5)$$

This definition of the SINR is often used in the beamforming literature [3]. The approximate evaluation (4) has the advantage that it only depends on the SINR in (5) and thus allows for a simple but approximate evaluation of the MI. In the Appendix, we provide an analysis of the error resulting from the approximate evaluation of the MI by a second-order multivariate Taylor series expansion.

C. Mutual Information as Performance Measure

The reason to use the MI (3) as performance measure lies in its generality. On the one hand, it can be interpreted as a constrained ergodic capacity over stationary and ergodic channels. On the other hand, it can be interpreted as a mean constrained capacity of a random constant-fading channel. The constraints are imposed by specifying the input as in Section II. We thus have a performance measure that has an interpretation in terms of an achievable rate for fast fading and slow fading channels. The relevance of an ergodic modeling of the channel is extensively discussed in [14].

We are interested in the evaluation of the performance over non-stationary channels; therefore, the MI in (3) will be time-dependent and does, strictly speaking, not have an interpretation as an achievable rate. However, non-stationary wireless channels are known to be DU [4], [13]; they can thus be assumed as coherent inside certain time (and frequency) regions and as stationary inside larger regions. In the fast fading case, coding can be performed inside a stationarity region; thus, (3) should be interpreted as the achievable rate over an equivalent stationary and ergodic channel with the statistics of that region. In the slow fading case, coding can be performed inside regions smaller than the coherence region. Therefore, (3) should be interpreted as a mean achievable rate over a random constant-fading channel. The correct interpretation in terms of fast or slow fading depends on the velocity of the MT and the (sufficiently long) coding length.

IV. CHANNEL MEASUREMENTS

The 3GPP LTE-relevant channel measurements were performed at 2.53 GHz in 2 bands of 45 MHz. The measurement campaign sequentially covers 3 BS positions with, amongst others, 25 m height in an urban macrocell scenario. In Fig. 1, an overview of the measurement environment in Ilmenau, Germany is shown. The 3 BS positions and the 3 MT reference tracks used in this paper are explicitly marked. We use a 20 MHz band at 2.505 GHz for the evaluations. At the BS, we choose a uniform linear array with the central 4 vertically polarized elements. The MT is a car driving with a maximal velocity of about 10 km/h. We extract 4 of the 12 vertically polarized elements of the lower uniform circular array at the MT to construct a MISO channel for each element. The elements correspond to the front (direction of motion), the back, and the two sides of the MT. For further details, see [4].
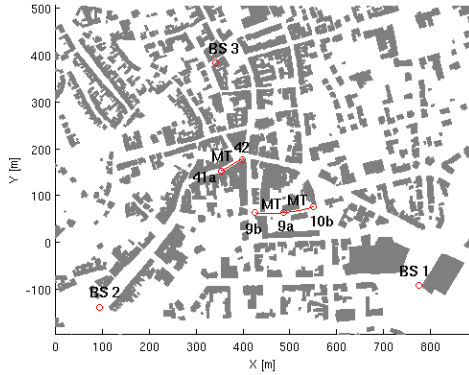
Fig. 1. Overview of the measurement environment with the 3 MT reference tracks and the 3 BS positions.

V. DATA PROCESSING

We preprocess the data by estimating a noise level in the time-delay domain and not considering any values below it. In order to estimate the statistical quantities, i.e., the MI and the correlation matrices, we approximate the ensemble averaging by an averaging over time and frequency. However, before doing so, we verify the DU assumption $\Delta\tau_{max}\Delta\nu_{max} \ll \tau_{max}\nu_{max} \ll 1$ to guarantee that the channel statistics can be estimated by averaging over time and frequency [13]. In [4], we showed that in our scenario the DU assumption is fulfilled with $\Delta\tau_{max}\Delta\nu_{max} \approx 1.16 \cdot 10^{-7}$ and $\tau_{max}\nu_{max} \approx 1.17 \cdot 10^{-4}$. Furthermore, we showed that an averaging in time over $N_t = 16$ and in frequency over $N_f = 128$ samples is a sensible choice to estimate the channel statistics. We thus average over a total of 2048 (≈ 500 non-coherent) realizations [4].

A. Channel Normalization

By studying different normalizations of the channel, we can get insight into different channel properties. Consider, e.g., the common approach of normalizing each channel realization. This effectively removes the path loss, the shadow fading, and the small-scale fading, and it is used to study the MIMO matrix structure only. We consider two different types of normalizations. On the one hand, we effectively remove the path loss and the shadow fading by normalizing the channel and setting constant transmitted powers at the BSs. The normalization is performed inside each time-frequency region used to estimate the statistics of the channel. This accounts for BSs that are able to adapt the transmitted power at certain intervals based on statistical knowledge of the channel. We denote this case by the term "per-interval channel normalization". On the other hand, we do not normalize the channel at all. Instead we set a common and constant transmitted power $\sigma_{x,i}^2[m] = \sigma_x^2$ at each BS i to reach a certain mean SNR over the whole track of the MT associated to BS k. This gives an understanding of the MI for the measured scenario as it is, without any adaptation of the TX power at the BSs over the MT track. We denote this case by the term "no channel normalization". $\overline{SNR}$ and $\overline{INR}$ are the mean of the instantaneous SNR and INR (2) averaged over 20 MHz in frequency and a certain time region, i.e., each interval for the per-interval channel normalization and the whole MT track in case of no channel normalization.

B. Sequential Measurements

The measurements of the individual BS-track links were performed sequentially. One resulting problem is that a perfect rerun of the tracks is not possible and will thus contain positioning errors. Another problem is that the channel can change in time even with no position errors. In order to reduce the errors due to the former problem, we match the positions of the measurements on each MT track for the different BSs. The position matching results in an error with mean 0.31 m and standard deviation 0.16 m. Note that we only evaluate statistical quantities, i.e., (3) and (4). Due to the DU property [13], the channel can be described by constant statistics inside some regions in time. Assuming that the matching ensures that the positioning errors remain inside such regions, we conclude the following. The MI (3) can be computed with sequential measurements if we assume the small-scale fading of the elements of $\mathcal{L}_{H,k}[m]$ as mutually independent; however, correlated shadow fading of the elements of $\mathcal{L}_{H,k}[m]$ is accounted for. The approximate evaluation of the MI relies on the mutual independency of the overall fading of the elements of $\mathcal{L}_{H,k}[m]$, but we will show that it is accurate. Note that by using the per-interval channel normalization only the small-scale fading is left. In [15], the reproducibility of large-scale parameters with sequential measurements is empirically demonstrated.

VI. RESULTS

In the following analysis, we associate track 10b-9a to BS 1, track 9a-9b to BS 2, and track 41a-42 to BS3. We study different orientations of the MTs, where all MTs have an equal orientation. The MT of BS k moves from the beginning to the end of the track, the positions of the outer-cell MTs w.r.t. BS k have fixed positions at the beginning, in the middle, and at the end of a track. The MI is given in bit/channel use (bit/c.u.), where a channel use corresponds to a time slot m in (1).

In Fig. 2, we see the cumulative distribution function (CDF) of the MI for the per-interval channel normalization with $\overline{SNR} = 10$ dB and different values of $\overline{INR}$. The MI of all MTs, orientations, and interferer positions is used to obtain the CDFs. Note that we have 2 BSs contributing each with $\overline{INR}$. Fig. 2 contains the MI (3) with and without ICI as well as the (linear) loss in MI due to ICI, i.e., the quotient of the MI without ICI and the MI with ICI. The dashed lines show the approximate (ap) evaluation of the MI, i.e., (4). As expected, with increasing $\overline{INR}$, the mean and the variance of the MI decrease and the mean and the variance of the loss in MI due to ICI increase. The variances are related to the correlation of the beamforming gains across the BSs. The approximate evaluation is very accurate in cell-edge scenarios, i.e., when signal and total ICI power are balanced, see Fig. 2 b) for $\overline{INR} = 5$ dB. In the case of no ICI, the approximation is an upper bound and thus not very accurate. When the ICI contribution is high, it slightly lower-bounds the MI, see Fig. 2 c) for $\overline{INR} = 10$ dB. The approximation is even more accurate when using cooperative beamforming techniques [16].

In Fig. 3, we show the evolution of the MI on track 10b-9a for the per-interval channel normalization with $\overline{SNR} = 10$ dB and $\overline{INR} = 10$ dB for each MT orientation. The outer-cell MTs are positioned at the end of their tracks. As a normalization
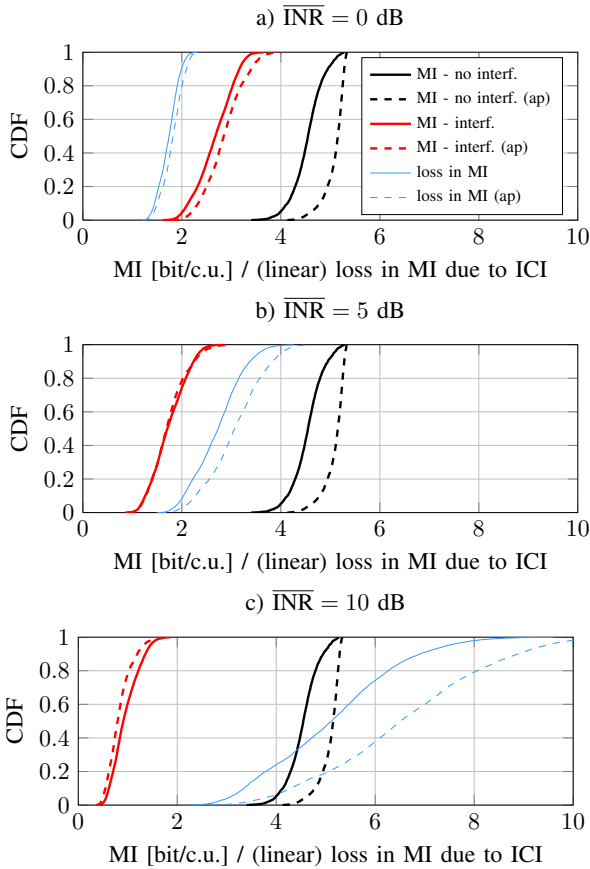
Fig. 2. CDF of the MI and the (linear) loss in MI due to ICI for $\overline{\mathrm{SNR}} = 10$ dB and the per-interval channel normalization.
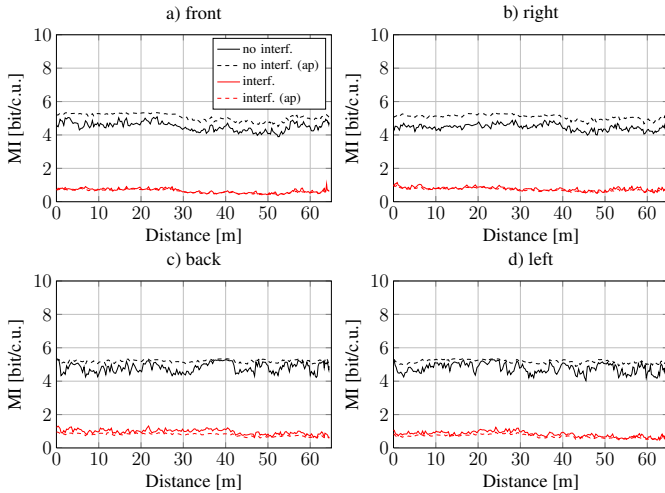

Fig. 3. MI for track 10b-9a with $\overline{\mathrm{SNR}} = 10$ dB, $\overline{\mathrm{INR}} = 10$ dB, the per-interval channel normalization, and the outer-cell MTs at the end positions.

of the channel is performed in each time interval, the path loss and the shadow fading are effectively removed, and the MI remains rather stable. The remaining variations in the MI are partly due to the use of statistical beamforming. Note that the variations of the MI are a manifestation of the non-stationarity of the channel. The corresponding figures for no channel normalization with $\overline{\mathrm{SNR}} = 10$ dB are shown in Fig. 4. Here, we observe the effects of path loss and shadow fading. On the first 25 m of the track where LOS occurs, high values
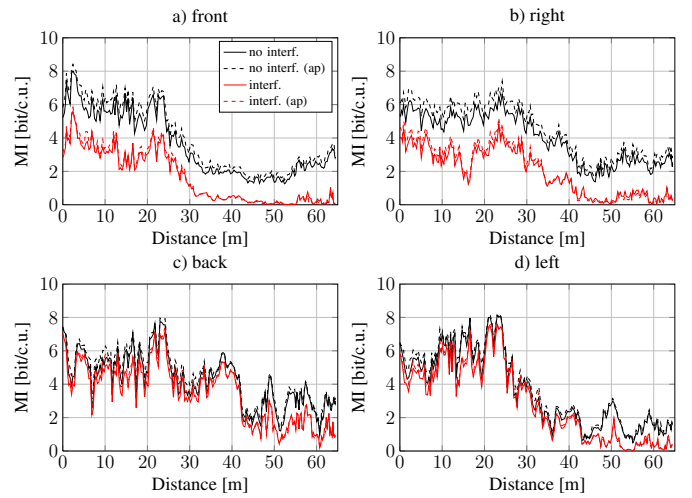

Fig. 4. MI for track 10b-9a with $\overline{\mathrm{SNR}} = 10$ dB, no channel normalization, and the outer-cell MTs at the end positions.

of the MI are observed. This is even the case when the MT antenna is oriented away from BS 1 as strong scattered paths are expected. The MI with ICI only degrades severely for the front and right orientation. This is due to the fact that, for the front and the right, higher channel gains are observed for the link from BS 3 [5]. Although not shown here, the positions of the outer-cell MTs do not significantly influence the MI on track 10b-9a. This is supported by the observation that the beamforming vectors are rather stable over the track [5].

In Table I, we provide the mean and the variance of the MI for each track and orientation of the MTs with $\overline{\mathrm{SNR}} = 10$ dB and different $\overline{\mathrm{INR}}$ in the case of the per-interval channel normalization. We observe low variances of the MI. The mean values of the MI without ICI are only slightly lower than the average values of the MI of approx. 5.5 bit/c.u. observed in 2x2 MIMO channels with equal power allocation in [11] and [17] for the same $\overline{\mathrm{SNR}}$; however, we use a different channel normalization. Table II gives the results for no channel normalization. Here, we observe that path loss and shadow fading lead to higher variances of the MI. Low mean values of the MI with ICI are observed on track 9a-9b due to the higher

TABLE I
MEAN AND VARIANCE OF THE MI WITH $\overline{\mathrm{SNR}} = 10$ dB, THE PER-INTERVAL CHANNEL NORMALIZATION, AND THE OUTER-CELL MTS AT THE END POSITIONS.

$\overline{\mathrm{INR}}$	Track	Mean (variance) of the MI [bit/c.u.]			
		front	right	back	left
$-\infty$ dB	10b-9a	4.51 (0.07)	4.45 (0.03)	4.82 (0.08)	4.75 (0.09)
	9a-9b	4.19 (0.11)	4.20 (0.08)	4.63 (0.03)	4.58 (0.03)
	41a-42	4.75 (0.06)	4.69 (0.05)	4.38 (0.05)	4.54 (0.04)
0 dB	10b-9a	2.25 (0.07)	2.42 (0.03)	2.77 (0.06)	2.55 (0.09)
	9a-9b	2.16 (0.04)	2.22 (0.04)	2.76 (0.05)	2.50 (0.02)
	41a-42	2.75 (0.03)	2.59 (0.03)	3.06 (0.02)	2.96 (0.02)
5 dB	10b-9a	1.33 (0.04)	1.50 (0.03)	1.78 (0.05)	1.57 (0.06)
	9a-9b	1.30 (0.02)	1.35 (0.02)	1.80 (0.04)	1.56 (0.02)
	41a-42	1.76 (0.02)	1.62 (0.02)	2.19 (0.02)	2.06 (0.02)
10 dB	10b-9a	0.65 (0.02)	0.77 (0.01)	0.96 (0.02)	0.80 (0.03)
	9a-9b	0.65 (0.01)	0.69 (0.01)	0.99 (0.02)	0.81 (0.01)
	41a-42	0.95 (0.01)	0.85 (0.01)	1.34 (0.02)	1.22 (0.01)

TABLE II
MEAN AND VARIANCE OF THE MI WITH $\overline{\text{SNR}} = 10$ dB, NO CHANNEL NORMALIZATION, AND THE OUTER-CELL MTS AT THE END POSITIONS.

$\overline{\text{INR}}$	Track	Mean (variance) of the MI [bit/c.u.]			
		front	right	back	left
$-\infty$ dB	10b-9a	3.48 (3.42)	3.87 (2.08)	4.09 (2.42)	3.36 (4.72)
	9a-9b	4.05 (0.72)	4.09 (0.60)	4.53 (0.43)	4.51 (0.33)
	41a-42	4.48 (1.00)	4.40 (0.93)	4.08 (1.27)	4.10 (1.66)
fixed by $\overline{\text{SNR}}$	10b-9a	1.47 (2.29)	1.82 (1.90)	3.27 (3.08)	2.62 (4.98)
	9a-9b	0.25 (0.04)	0.21 (0.02)	0.23 (0.01)	0.14 (0.01)
	41a-42	2.81 (0.78)	2.57 (0.76)	2.80 (0.68)	2.96 (0.98)

distance and thus higher path loss from BS 2 than from the other BSs. At the beginning of track 9a-9b, the distance to BS 2 is about 100 m larger than to BS 1 and 3.

VII. CONCLUSION

We have characterized the achievable performance in a downlink beamforming scenario with ICI and SUD. The analysis is based on measurements in an urban macrocell scenario at 2.53 GHz. We introduced the MI as performance measure for fast and slow fading channels that are non-stationary but DU. We evaluated the MI with and without ICI for two types of channel normalization. The measured values can be used for a comparison to results obtained from simulations, and they can serve as baseline to study the performance improvements of beamforming techniques for ICI mitigation. Furthermore, by a second-order multivariate Taylor series expansion, we analyzed an approximate evaluation of the MI that allows for a simple analysis; it is accurate in realistic ICI scenarios.

APPENDIX

The approximation of the MI in (4) is based on Jensen's inequality; more specifically, an upper- and a lower-bounding step are performed [10]. We define the signal and ICI contributions normalized to the noise variance as

$$a[m] = \mathbf{L}_{\text{H},k}[m]\mathbf{Q}_k[m]\mathbf{L}_{\text{H},k}^H[m]/\sigma_n^2 \quad (6)$$

$$b[m] = \sum_{i=1, i\neq k}^{N_{\text{BS}}} \mathbf{L}_{\text{H},k,i}[m]\mathbf{Q}_i[m]\mathbf{L}_{\text{H},k,i}^H[m]/\sigma_n^2. \quad (7)$$

The approximation error $\Delta I_{\text{BF}}(a[m], b[m])$, i.e., the difference between (4) and (3), can be characterized by a second-order multivariate Taylor series expansion at $\text{E}\{a[m]\}$ and $\text{E}\{b[m]\}$ if $a[m]$ and $b[m]$ are close to their expected values. For convenience, we use the natural logarithm $\ln(x) = \log(x)/\log(e)$, and we omit the time argument m in the subsequent analysis.

$$\ln\left(1 + \frac{a}{b+1}\right) \approx \ln\left(1 + \frac{\text{E}\{a\}}{\text{E}\{b\}+1}\right)$$
$$+ (a - \text{E}\{a\}) \frac{1}{\text{E}\{a\} + \text{E}\{b\} + 1}$$
$$- (b - \text{E}\{b\}) \frac{\text{E}\{a\}}{(\text{E}\{b\}+1)(\text{E}\{a\}+\text{E}\{b\}+1)}$$
$$- \frac{(a - \text{E}\{a\})^2}{2} \frac{1}{(\text{E}\{a\}+\text{E}\{b\}+1)^2}$$
$$+ \frac{(b - \text{E}\{b\})^2}{2} \frac{\text{E}\{a\}(\text{E}\{a\}+2\,\text{E}\{b\}+2)}{(\text{E}\{b\}+1)^2(\text{E}\{a\}+\text{E}\{b\}+1)^2}$$

$$- (a - \text{E}\{a\})(b - \text{E}\{b\}) \frac{1}{(\text{E}\{a\}+\text{E}\{b\}+1)^2}. \quad (8)$$

It follows that $\Delta I_{\text{BF}}(a, b)$ is approximately given by

$$\frac{\Delta I_{\text{BF}}(a, b)}{\log(e)} = \ln\left(1 + \frac{\text{E}\{a\}}{\text{E}\{b\}+1}\right) - \text{E}\left\{\ln\left(1 + \frac{a}{b+1}\right)\right\}$$
$$\approx + \frac{\text{var}\{a\}}{2} \frac{1}{(\text{E}\{a\}+\text{E}\{b\}+1)^2}$$
$$- \frac{\text{var}\{b\}}{2} \frac{\text{E}\{a\}(\text{E}\{a\}+2\,\text{E}\{b\}+2)}{(\text{E}\{b\}+1)^2(\text{E}\{a\}+\text{E}\{b\}+1)^2}$$
$$+ \text{cov}\{a, b\} \frac{1}{(\text{E}\{a\}+\text{E}\{b\}+1)^2}. \quad (9)$$

For mutually uncorrelated a and b, (9) is composed of the first two terms only; they contribute with opposite signs and can cancel each other out. In the ICI-free case, only the first term remains and thus a positive error results.

REFERENCES

[1] D. Gesbert *et al.*, "Multi-cell MIMO cooperative networks: A new look at interference," *IEEE J. Sel. Areas Commun.*, vol. 28, no. 9, pp. 1380–1408, Dec. 2010.

[2] M. Schubert and H. Boche, "Solution of the multiuser downlink beamforming problem with individual SINR constraints," *IEEE Trans. Veh. Technol.*, vol. 53, no. 1, pp. 18–28, Jan. 2004.

[3] M. Kobayashi and G. Caire, "Joint beamforming and scheduling for a multi-antenna downlink with imperfect transmitter channel knowledge," *IEEE J. Sel. Areas Commun.*, vol. 25, no. 7, pp. 1468–1477, Sep. 2007.

[4] A. Ispas, C. Schneider, G. Ascheid, and R. Thomä, "Analysis of local quasi-stationarity regions in an urban macrocell scenario," in *Proc. 71st IEEE Veh. Technol. Conf. (VTC)*, Taipei, Taiwan, May 2010.

[5] ——, "On non-stationary urban macrocell channels in a cooperative downlink beamforming scenario," in *Proc. 72nd IEEE Veh. Technol. Conf. (VTC)*, Ottawa, Canada, Sep. 2010.

[6] P. Almers *et al.*, "Survey of channel and radio propagation models for wireless MIMO systems," *EURASIP J. Wireless Commun. Netw.*, vol. 2007, no. 1, Jan. 2007.

[7] IST-4-027756 WINNER II D1.1.2 V1.2. (2008, Feb.) WINNER II channel models. [Online]. Available: http://www.ist-winner.org

[8] COST 2100, Special Interest Group A. (2011, Jan.) COST 2100 reference scenarios. [Online]. Available: http://grow.lx.it.pt/web/cost2100/

[9] R. S. Blum, "MIMO capacity with interference," *IEEE J. Sel. Areas Commun.*, vol. 21, no. 5, pp. 793–801, Jun. 2003.

[10] G. Taricco and E. Riegler, "On the ergodic capacity of the asymptotic separately-correlated Rician fading MIMO channel with interference," in *Proc. IEEE Int. Symp. Information Theory (ISIT)*, Nice, France, Jun. 2007, pp. 531–535.

[11] S. Jaeckel, L. Thiele, and V. Jungnickel, "Interference limited MIMO measurements," in *Proc. 71st IEEE Veh. Technol. Conf. (VTC)*, Taipei, Taiwan, May 2010.

[12] E. Björnson, M. Bengtsson, and B. Ottersten, "Optimality properties and low-complexity solutions to coordinated multicell transmission," in *Proc. IEEE Global Commun. Conf. (GLOBECOM)*, Miami, FL, USA, Dec. 2010.

[13] G. Matz, "On non-WSSUS wireless fading channels," *IEEE Trans. Wireless Commun.*, vol. 4, no. 5, pp. 2465–2478, Sep. 2005.

[14] N. Jindal and A. Lozano, "Fading models and metrics for contemporary wireless systems," in *Proc. 44th Asilomar Conf. Signals, Syst., Comput.*, Pacific Grove, CA, USA, Nov. 2010, pp. 625–629.

[15] M. Narandžić *et al.*, "Variation of estimated large-scale MIMO channel properties between repeated measurements," in *Proc. 73rd IEEE Veh. Technol. Conf. (VTC)*, Budapest, Hungary, May 2011.

[16] A. Ispas, C. Schneider, G. Ascheid, and R. Thomä, "Analysis of mismatched downlink beamforming over non-stationary channels with interference," in *Proc. XXX General Assembly and Scientific Symp. of the Int. Union of Radio Science (URSI)*, Istanbul, Turkey, Aug. 2011, (invited paper).

[17] D. Chizhik *et al.*, "Multiple-input-multiple-output measurements and modeling in Manhattan," *IEEE J. Sel. Areas Commun.*, vol. 21, no. 3, pp. 321–331, Apr. 2003.